A Na^+ Channel Mutation Linked to Hypokalemic Periodic Paralysis Exposes a Proton-selective Gating Pore

Arie F. Struyk[1] and Stephen C. Cannon[1,2]

[1]Department of Neurology and [2]Program in Neuroscience, University of Texas-Southwestern Medical Center, Dallas, TX 75390

The heritable muscle disorder hypokalemic periodic paralysis (HypoPP) is characterized by attacks of flaccid weakness, brought on by sustained sarcolemmal depolarization. HypoPP is genetically linked to missense mutations at charged residues in the S4 voltage-sensing segments of either CaV1.1 (the skeletal muscle L-type Ca^{2+} channel) or NaV1.4 (the skeletal muscle voltage-gated Na^+ channel). Although these mutations alter the gating of both channels, these functional defects have proven insufficient to explain the sarcolemmal depolarization in affected muscle. Recent insight into the topology of the S4 voltage-sensing domain has aroused interest in an alternative pathomechanism, wherein HypoPP mutations might generate an aberrant ionic leak conductance by unblocking the putative aqueous crevice ("gating-pore") in which the S4 segment resides. We tested the rat isoform of NaV1.4 harboring the HypoPP mutation R663H (human R669H ortholog) at the outermost arginine of S4 in domain II for a gating-pore conductance. We found that the mutation R663H permits transmembrane permeation of protons, but not larger cations, similar to the conductance displayed by histidine substitution at Shaker K^+ channel S4 sites. These results are consistent with the notion that the outermost charged residue in the DIIS4 segment is simultaneously accessible to the cytoplasmic and extracellular spaces when the voltage sensor is positioned inwardly. The predicted magnitude of this proton leak in mature skeletal muscle is small relative to the resting K^+ and Cl^- conductances, and is thus not likely to fully account for the aberrant sarcolemmal depolarization underlying the paralytic attacks. Rather, it is possible that a sustained proton leak may contribute to instability of V_{REST} indirectly, for instance, by interfering with intracellular pH homeostasis.

The Journal of General Physiology

INTRODUCTION

Hypokalemic periodic paralysis is a heritable disorder of skeletal muscle, exhibiting an autosomal dominant mode of transmission, manifested clinically as episodic attacks of flaccid paralysis accompanied by hypokalemia. The paralytic attacks are the consequence of sustained depolarization of the sarcolemmal resting potential (V_{REST}), rendering the muscle fibers electrically inexcitable (for a review see Cannon, 2006). The cause of this aberrant depolarization is not known, nor is the origin of the characteristic hypokalemia during the attacks. Genetic linkage of the disorder has been established in a majority of hypokalemic periodic paralysis (HypoPP) kindreds to mutations in either the *CACNA1S* or *SCN4A* genes, encoding the ion channels CaV1.1 (skeletal muscle L-type Ca^{2+} channel) and NaV1.4 (skeletal muscle voltage-gated Na^+ channel), respectively (Jurkat-Rott et al., 1994; Ptacek et al., 1994; Bulman et al., 1999; Jurkat-Rott et al., 2000). CaV1.1 and NaV1.4 share structural homology; both are organized into four large domains (DI–DIV), which in turn are composed of six membrane-spanning peptide segments, denoted S1–S6 (for review see Catterall, 1995). Mutations causing HypoPP uniformly introduce missense substitutions at positively charged residues in S4 segments spread throughout either channel (Jurkat-Rott et al., 1994; Ptacek et al., 1994; Bulman et al., 1999; Jurkat-Rott et al., 2000; Sternberg et al., 2001; Carle et al., 2006). These positive charges are critical to channel function by mediating S4 segment translocation in response to changes in membrane potential, thereby conferring voltage sensitivity to gating of the central Na^+ conducting pore.

The revelation that HypoPP is caused by alterations to voltage sensing segments has led many to hypothesize that the pathological effect of these mutations is due to loss of normal S4 function, manifest as impaired gating of CaV1.1 or NaV1.4. For mutations in CaV1.1, various functional defects have been reported, including shifts in the voltage dependence of activation and inactivation (Lerche et al., 1996), slowed activation kinetics (Morrill et al., 1998), and reduced CaV1.1 current density (Lapie et al., 1996). Speculation has thus arisen that alterations in Ca^{2+} flux and its effect on internal Ca^{2+} homeostasis might contribute to the development of paralytic attacks. HypoPP mutations in NaV1.4 uniformly enhance channel inactivation, by impeding recovery from either fast- or slow-inactivation states (Jurkat-Rott et al., 2000; Struyk et al., 2000; Kuzmenkin et al., 2002; Carle et al., 2006). These results have led investigators to suggest that reduced Na^+ channel availability might also predispose to

Correspondence to Arie F. Struyk: arie.struyk@utsouthwestern.edu

Abbreviations used in this paper: HB, high-buffer; HypoPP, hypokalemic periodic paralysis; WT, wild-type.

paralytic attacks. Neither of these hypotheses, however, offers a satisfactory explanation for core phenotypic features of HypoPP, such as the sarcolemmal depolarization and hypokalemia, nor for the apparent singular requirement for S4 charge-altering mutations to induce the disorder.

Recent insight into the topology of the canonical voltage-sensing domain shared by many voltage-gated channels has established a foundation for an alternative pathophysiological hypothesis. In a growing number of ion channels, missense substitution of charged S4 side chains is able to establish an accessory ionic permeation pathway separate from the central ion-conducting pore (Starace et al., 1997; Starace and Bezanilla, 2001, 2004; Sokolov et al., 2005; Tombola et al., 2005). The permeation mechanisms thus established differ in ionic selectivity and voltage dependence, depending on the site and nature of the side chain substitution. These observations support a structural model in which S4 segments reside in water-filled crevices penetrating deeply into the lipid bilayer. Growing evidence suggests that these putative "gating pores" are characterized by a focal constriction, which is normally occupied by charged side chains of the resident S4 segment, thereby preventing aqueous continuity between the intra- and extracellular compartments (Starace and Bezanilla, 2004).

These findings have provoked speculation that HypoPP mutations might similarly foster an aberrant ionic conductance flowing through a structural defect in a CaV1.1 or NaV1.4 gating pore. In this manner, equivalent pathological conductances mediated by mutations in structural elements shared by both channels might thereby account for the common downstream phenotype, separate from the effects individual mutations might exert on channel gating. An aberrant current consistent with a gating pore leak has recently been reported by Sokolov et al. (2007) who demonstrated a current with limited selectivity among monovalent cations in the R666G HypoPP mutation in the rat isoform of NaV1.4 (R672G ortholog). A current with similar voltage dependence was demonstrated in the R663H and R666H mutations (R669H and R672H equivalents), which the authors attributed to a Na^+ ion leak. These results have lent strong support to the hypothesis that an aberrant gating pore current may contribute to the pathophysiology of HypoPP.

In experiments using the rat isoform of NaV1.4, we also found that the missense substitution R663H fosters ionic permeation through a presumptive transmembrane gating pore, resulting in a current exhibiting similar voltage dependence as that reported by Sokolov et al. In contrast to that report, however, the bulk of the R663H-associated current we detected is carried by protons. Larger, physiologically abundant monovalent and divalent cations, including Na^+, were not permeant charge carriers. Due to its small amplitude, an aberrant proton conductance such as that flowing through the exposed R663H gating pore is unlikely to exert a significant direct depolarizing influence over sarcolemmal V_{REST}. A plausible alternative mechanism is discussed, whereby HypoPP mutants might introduce a persistent proton leak across the sarcolemma, potentially impairing the stability of V_{REST} indirectly via effects on myoplasmic pH.

MATERIALS AND METHODS

Expression of Nav1.4 Channels

The rat adult skeletal muscle Na^+ channel α-subunit cDNA (rNaV1.4) subcloned into the EcoRI site of the *Xenopus* expression vector pGEMHE (Liman et al., 1992) was used as a template for site-directed mutagenesis using the QuickChange Mutagenesis kit (Stratagene). Primers were designed to alter codons specifying the substitution mutation and to introduce a translationally silent restriction site to facilitate rapid screening by restriction digest. Point mutations were confirmed by direct sequencing through the codon position.

cRNA was synthesized by in vitro transcription using the mMessage mMachine kit, (Ambion) from 2 μg of each expression construct linearized with NheI.

X. laevis were housed in an AAALAC-accredited facility, and all experiments were performed within guidelines established by the UTSW Institutional Animal Care and Use Committee. *Xenopus* oocytes between 1–7 d post-harvest were injected with ∼50 ng of cRNA encoding either wild-type (WT) or mutant NaV1.4 protein, along with ∼50 ng (approximately twofold molar excess) of cRNA encoding the β1-subunit. Injected oocytes were incubated between 1 and 5 d at 17°C in ND96 medium (in mM: 96 NaCl, 2 KCl, 1.8 $CaCl_2$, 1 $MgCl_2$, 5 HEPES, pH 7.6) supplemented with 2.5 mg/ml pyruvate and 50 μg/ml gentamicin.

Electrophysiology

In all experiments, oocytes were voltage-clamped in the cut-open configuration, with active clamp of the upper and guard compartments, controlled by a CA-1B amplifier (Dagan Corporation), using the mainframe clamp circuitry. The lower oocyte membrane was permeabilized with 0.1% saponin to gain low-resistance electrical access to, and facilitate ionic control over, the intracellular compartment. The amplifier was controlled and signals recorded with a Pentium-3 based PC running pClamp 7 software, interfaced using a DigiData 1200 A/D converter (Molecular Devices).

Voltage-sensing electrodes were fabricated from borosilicate capillary glass (1.5 mm OD thin wall with filament; WPI), using a multi-stage puller (Sutter Instrument Co.), and were filled with 3M KCl. Tip resistances were between 0.2 and 2 MΩ. The leads of the amplifier headstage, attached to Ag^+/AgCl pellets in plastic wells containing 1 M NaCl solution, were connected to the upper, guard, and lower oocyte compartments using glass agarose bridges containing 110 mM Na^+-methanesulfonate, 10 mM HEPES, pH 7.4, and threaded with platinum wire. No analogue correction of capacitance or linear leak currents was applied during the experiments.

Current signals were filtered with an external device (Frequency Devices). Signals were filtered at 10 kHz and sampled at 100 kHz for Na^+ channel gating currents, or filtered at 1 kHz and sampled at 5 kHz for gating pore leakage currents. For gating current measurements, a P/−8 subtraction protocol was used to subtract linear leak and capacitance current from a holding potential of −130 mV. No on-line leak subtraction was applied to measurements of gating pore leak currents; rather, passive membrane leak conductance was identified and subtracted off-line as described below.

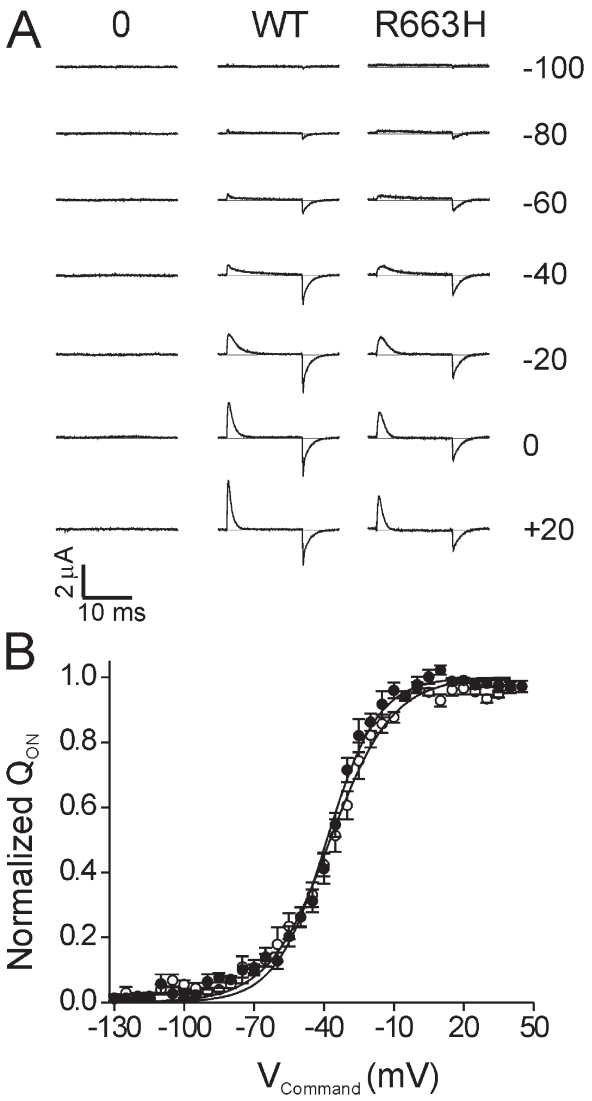

Figure 1. Gating charge displacement of rNaV1.4 WT and R663H channels. Oocytes were held at −100 mV, and gating charge displacement was determined by a series of 15-ms voltage commands between −130 and +40 mV in 5-mV increments, following a 15-ms prepulse to −130 mV. Linear leak and capacitance currents were subtracted by a P/−8 protocol from −130 mV. Bath solutions contained TEA^+ as the predominant cation. Representative gating currents are displayed in A, for a mock-injected oocyte (0), and oocytes expressing WT or R663H channels (denoted at top). Command voltages eliciting the currents in each trace are displayed at the right. The voltage dependence of normalized Q_{On} charge displacement is shown in B, for WT channels (open circles, $n = 8$), and R663H mutants (filled circles, $n = 7$). Curves are fit with a Boltzmann function yielding the following values: WT, $V_{1/2} = -37.3 \pm 2.4$ mV, $k = 13.3 \pm 0.6$ mV; and R663H, $V_{1/2} = -38.7 \pm 1.9$ mV, $k = 11.0 \pm 0.6$ mV).

All experiments used Cl^--free solutions to minimize contamination with endogenous oocyte Cl^- currents. Solutions for electrophysiological recording were as follows. For initial experiments characterizing the amplitude, voltage dependence, and ionic permeability of gating-pore currents, the external solution (applied to the external and guard compartments) contained (in mM) 115 TEA-OH (or, for later experiments, equimolar amounts of NaOH, KOH, or $NMDG^+$), 1.5 $CaOH_2$, 1 $MgOH_2$, 10 HEPES, pH 7.4 with methanesulfonic acid. Internal solution contained (in mM) 115 CsOH, 10 EGTA, 10 HEPES, pH 7.4 with methanesulfonic acid. For isolated characterization of proton currents requiring manipulation of the pH gradient, solutions were prepared following protocols using high-buffer (HB) solutions reported in Starace and Bezanilla (2001). External HB solution contained (in mM) 78 Tris, 178 HEPES, 1.5 $CaOH_2$, and 1 $MgOH_2$ (pH 7.4). Internal HB solutions contained (in mM) 2 mM EGTA, and either 236 MES with 17 $NMDG^+$ (for pH 5.0), 150 HEPES with 68 $NMDG^+$ (for pH 7.4), or 45 CHES with 180 $NMDG^+$ (for pH 9.0). All bath solutions contained 1 μM tetrodotoxin (Sigma-Aldrich) to block ionic currents through the central pore. The osmotic activity of the different recording solutions was measured and found to fall within a range of 30 mOsm.

Recordings were not begun until >30 min after permeabilization of the oocyte membrane, to allow for equilibration of the intracellular compartment with the lower bath. Intracellular pH was not measured directly.

Data Analysis

Data was analyzed using a combination of ClampFit 9 (Molecular Devices), Excel (Microsoft), and OriginPro 6.1 (OriginLab) software packages. For gating currents, Q_{On} was measured by integration of the leak-corrected current transient recorded over a 15-ms voltage step. To compensate for the presence of small leak subtraction errors arising from the combination of linear nonspecific leak and nonlinear gating pore conductance, the steady-state current recorded during the last 0.5 ms of the voltage step in each trace was subtracted from the full current record before integration. The Q_{On}-V relationship was then determined by normalizing charge movement to the maximal charge displacement at saturating voltages ($Q_{On,Max}$), derived from fits with the Boltzmann function:

$$Q_{On} = \frac{Q_{On,Max}}{\left[1 + e^{-\left(\frac{V - V_{1/2}}{k}\right)}\right]},$$

where $V_{1/2}$ is the voltage of half-maximal charge movement and k is the slope.

Steady-state leak currents, composed of ionic currents permeating the rNaV1.4 gating-pore and residual nonspecific leak across the oocyte membrane, were measured as the mean current elicited during the last 100 ms of a 300-ms voltage command. When subtraction of nonspecific membrane leak currents was desirable, it was accomplished off-line by subtracting the mean leak current from a pooled population of mock-injected oocytes recorded in the same bathing and intracellular solutions as the test population.

The conductance characteristics of the outward R663H proton current, G_{Max}, in Fig. 5 were determined by fitting the leak-corrected current amplitudes to a modified Boltzmann function:

$$I = \frac{G_{Max} \times \left(V - E_{Rev,H+}\right)}{\left[1 + e^{-\left(\frac{V - V_{1/2}}{k}\right)}\right]},$$

where $V_{1/2}$ is the voltage of half-maximal activation, k is the slope, and $E_{Rev,H+}$ is the proton reversal potential of the current determined for each oocyte. Conductance values at each voltage tested were then normalized to G_{Max} to determine relative open probability. Error bars in all figures represent ± SEM.

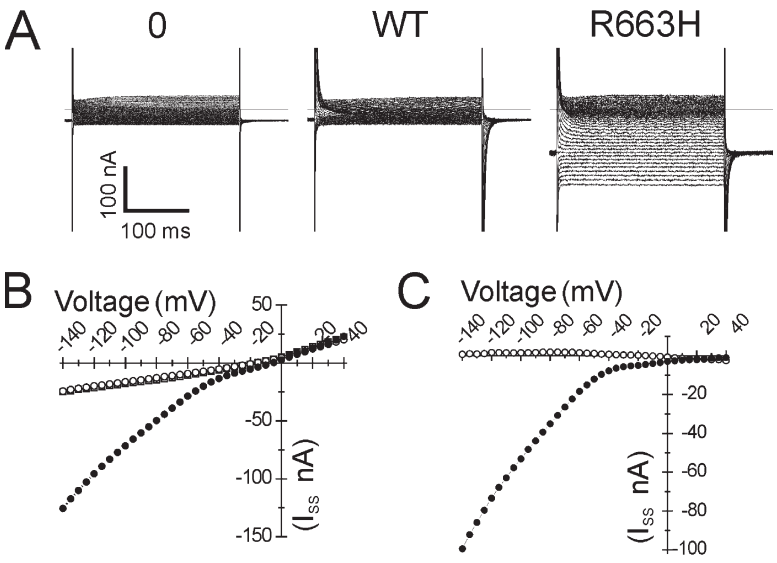

Figure 2. R663H channels are associated with an aberrant inward current. In A, representative steady-state current responses to 300-ms voltage commands between −140 and +30 mV from a holding potential of −100 mV are shown, for mock-injected oocytes (0), or oocytes expressing WT or R663H channels (denoted at top; recordings are from the same oocytes whose gating charge movement is depicted in Fig. 1 A). The mean steady-state current during the last 100 ms of the command pulse is plotted versus voltage in B, for mock-injected (open squares, lying beneath WT points), WT- (open circles), and R663H-expressing oocytes (filled circles). The R663H-expressing oocyte exhibits a hyperpolarization-induced inward current not observed in the WT expressing oocyte. C depicts the R663H and WT-associated currents (same data as in B) after subtraction of the mean nonspecific leak from a pooled population of mock-injected oocytes.

RESULTS

The ortholog of the most prevalent human HypoPP mutation in NaV1.4 (R669H) (Bulman et al., 1999; Sternberg et al., 2001) was introduced into the rat isoform of the skeletal muscle Na^+ channel (rNaV1.4-R663H) (Trimmer et al., 1989). This mutation replaces the outermost charged residue in the DIIS4 segment. Freshly harvested *Xenopus* oocytes were coinjected with RNA encoding mutant or WT channels along with the β1-subunit (McClatchey et al., 1993). Gating and ionic currents were recorded using the cut-open oocyte voltage clamp method. All recordings were made in the presence of 1 μM tetrodotoxin to block ionic currents through the central Na^+ channel pore.

Large currents arising from Na^+ channel gating charge displacement could be detected within 3 d after RNA injection. Representative gating currents after subtraction of linear capacitance and leak components are shown in Fig. 1 A, for oocytes injected with WT and R663H mutant RNAs, as well as a mock-injected oocyte for comparison. No significant difference was detected in the voltage dependence of depolarization-provoked charge displacement ($Q_{On(V)}$) between R663H and WT channels (Fig. 1 B), both of which are consistent with the characteristic NaV1.4 $Q_{On(V)}$ relationship described by others (Cha et al., 1999).

Low amplitude leak conductances were characteristic of both WT- and R663H-expressing oocytes. At high amplifier gain, however, a marked difference between leak currents in oocytes expressing WT versus R663H channels could be discerned. Examples of these leak currents are displayed in Fig. 2 A, recorded from the same oocytes whose charge movement is depicted in Fig. 1 A. A small, persistent, inwardly rectifying current is noted in R663H-expressing oocytes, which diverges from the nonspecific leak in mock-injected and WT-expressing oocytes at hyperpolarized potentials. There was no difference in the steady-state currents between oocytes expressing WT and R663H channels at depolarized voltages, indicating that opening of the R663H-associated leak conductance is favored by membrane potentials <-40 mV. The amplitudes of the R663H-associated inward currents recorded at −140 mV were only ∼5% of peak gating current amplitudes in the corresponding oocytes. Peak gating currents of NaV1.4 channels are ∼50 times smaller than corresponding ionic currents flowing through the central pore (Armstrong and Bezanilla, 1974); thus the relative amplitude of the R663H-associated current at −140 mV was estimated to be ∼0.1% of the peak ionic currents in physiological Na^+ gradients.

This aberrant inward current was not carried by the central ion-conducting pore of rNaV1.4, as the pore was maximally blocked with tetrodotoxin, and furthermore the conductance was activated by hyperpolarization to voltages at which the opening of the central pore was not favored. We propose that the R663H-associated inward current arose from exposure of an accessory ionic permeation pathway through the water-filled crevice housing the mutant DIIS4 segment (e.g., an exposed gating-pore). If so, then the voltage dependence of the R663H-associated current would reflect its dependence on the positioning of the DIIS4 voltage sensor. Opening of the R663H conductance would be promoted by inward positioning of the DIIS4 segment favored by hyperpolarization, whereas the absence of aberrant R663H currents at depolarized voltages would reflect closure of the permeation pathway by translocation of the DIIS4 to its outward, "activated" orientation. The amplitude and directionality of the current flow would therefore depend on the driving force of the permeant ions relative to membrane voltages at which the putative R663H

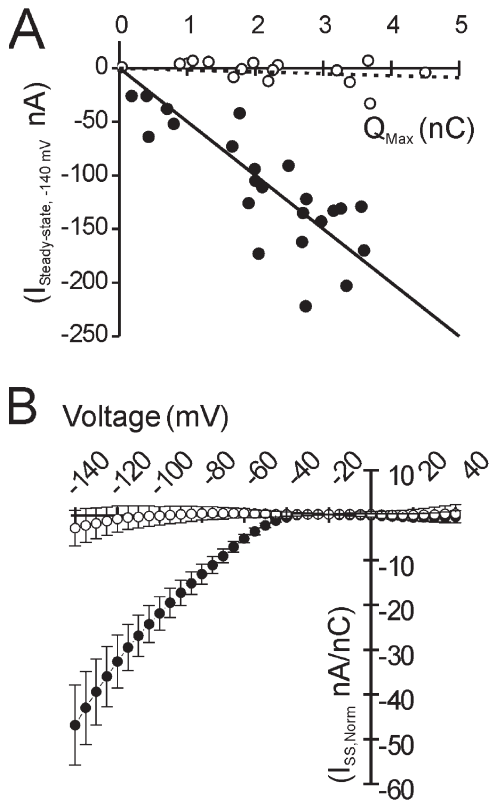

Figure 3. R663H channels are the origin of the aberrant inward current. In A, the nonspecific leak from a pooled population of mock-injected oocytes was subtracted from steady-state currents from both WT- and R663H-expressing oocytes. The leak-corrected current amplitudes elicited by the −140 mV command voltage are plotted against maximal gating charge displacement for individual oocytes expressing WT (open circles) or R663H channels (filled circles). Linear fits to the data are overlaid. The amplitude of the nonlinear, inward current scales with increased R663H channel expression (black line), whereas no aberrant inward current is evident in oocytes expressing comparable levels of WT channels (dotted line). In B, this scaling is used to normalize current amplitudes from different oocytes to corresponding $Q_{on,Max}$, to facilitate comparison across oocyte populations exhibiting different levels of Na^+ channel expression. A prominent inward current is characteristic of R663H-expressing oocytes (filled circles), whereas there is little aberrant inward current in WT-expressing oocytes (open circles).

gating pore was open (e.g., <-40 mV). Thus, the inward direction of the aberrant R663H current in Fig. 2 (A and B) was most likely to reflect permeation of cations (given the substitution of anions with methanesulfonate) subject to an inward driving force at hyperpolarized membrane voltages. To fully test this hypothesis, we characterized both the relative ionic selectivity and gating characteristics of the R663H-associated conductance in greater detail.

Initially, we sought a method to isolate the R663H-associated conductance from the nonspecific leak of the oocyte membrane. In most oocytes, the magnitude of the R663H-associated conductance was only two to three times the amplitude of the nonspecific oocyte leak. No ionic or pharmacological blockers of the R663H-associated currents could be identified, including millimolar concentrations of Ni^+, Cd^{2+}, and Li^+. Furthermore, estimation of the nonspecific leak from membrane responses recorded at depolarized voltages (where the putative R663H gating pore appeared to be closed) was confounded by nonlinearity over much of the voltage range. Therefore, the oocyte leak conductance was assessed in a population mean of mock-injected oocytes, and this template was used as the nonspecific leak for subtraction from individual oocytes expressing WT and R663H channels. Similar results were obtained by linear extrapolation of the nonspecific leak recorded at depolarized potentials, but the superior compensation for the nonlinearity by subtraction of the mean leak resulted in better segregation of the R663H-associated and nonspecific components of the current. Currents isolated in this manner are dominated by the R663H-specific component (Fig. 2 C).

To support the contention that the aberrant inward current originates from R663H mutant channels, we tested whether the amplitude of the R663H-associated current scaled with the level of R663H channel expression, as measured by $Q_{On,Max}$. A robust correlation between inward current amplitudes and the corresponding maximal gating charge displacement in several individual oocytes is evident in Fig. 3 A. Conversely, no inward current was detected in WT-expressing oocytes selected for similar levels of Na^+ channel expression. To facilitate the comparison of currents between oocytes with different rNaV1.4 expression levels, leak-subtracted currents were normalized to maximal gating charge displacement in the corresponding oocyte. Normalized, leak-corrected currents are depicted in Fig. 3 B from populations of WT- and R6663H-expressing ooctyes, demonstrating the mean hyperpolarization-activated current associated with R663H channels.

Ionic substitution experiments were performed to identify the relative ionic selectivity of this hyperpolarization-activated R663H conductance. Normalized R663H current amplitudes recorded in bath solutions containing either Na^+, K^+, or $NMDG^+$ as the predominant extracellular cation were not significantly different than normalized currents recorded in TEA^+-containing bath solutions (Fig. 4 A). In similar experiments (not depicted), normalized currents were not altered after substitution of trace divalent cations with Ba^{2+}. The lack of variability in normalized current amplitude despite large size differences among the ionic species in each experiment strongly suggested that none of these cations were permeant charge carriers. A consistent feature of each experiment, however, was the free H^+ concentration (pH) of the different recording solutions, raising the possibility that the R663H current was due to selective permeation of protons. This possibility was consistent with published reports demonstrating that exposed gating-pores arising from histidine-substituted S4 side chains in *Shaker* K^+

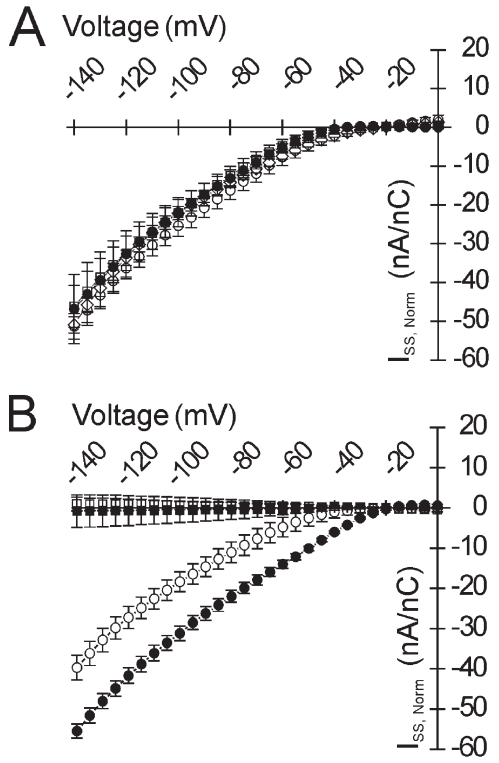

Figure 4. The R663H-associated gating pore is impermeable to large cations, but permissive for protons. The selectivity of R663H-associated currents for different cations was assessed. In all experiments, leak subtraction was achieved as in Fig. 2 B, using nonspecific leak currents derived from pooled data from mock-injected oocytes exposed to the same ionic conditions as the experimental group. The current–voltage relationship of R663H-specific currents, normalized to maximal Q_{On} as in Fig. 3 B, is plotted in A. Normalized R663H gating-pore currents measured with TEA^+ as the external cation (filled circles, same data as in Fig. 2 C for reference), is not significantly different from normalized current densities recorded in external K^+ (open circles, $n = 6$), Na^+ (open diamonds, $n = 5$), or $NMDG^+$ (open squares, $n = 5$). The selectivity of the hyperpolarization-activated R663H conductance for protons was assessed in experiments depicted in B, by manipulating the proton driving force through changes in the transmembrane pH gradient. This was accomplished by buffering the intracellular pH to different values while the extracellular pH was kept constant at 7.4. The R663H current density exhibits the same directionality and amplitude as the densities in A when the pH gradient is symmetric (intracellular pH 7.4, open circles). When the proton driving force was increased at hyperpolarized voltages by buffering the intracellular pH to 9.0, the normalized R663H-associated inward currents increased (filled circles). No aberrant inward current was observed in WT-expressing oocytes when the intracellular pH was either 7.4 (open squares) or 9.0 (filled squares).

channels are predominantly selective for protons over other cations (Starace et al., 1997; Starace and Bezanilla, 2001; Tombola et al., 2005).

To test the proton selectivity of the R663H gating-pore, the proton driving force was manipulated by shifting the reversal potential, E_{H+}, through alterations of the transmembrane pH gradient. If the R663H-associated conductance is carried by H^+, then altering the proton driving force should result in shifts in the amplitude and directionality, but not voltage dependence, of the R663H currents. To accomplish this, oocytes were bathed in different "high-buffer" recording solutions, similar to those used by Starace and Bezanilla (2001), enabling stringent control over both the intra- and extracellular pH. The extracellular pH was maintained at 7.4 for all experiments. In initial experiments, the proton concentrations on both sides of the membrane were set as equivalent, by buffering the intracellular compartment to pH 7.4 ($E_{H+} = 0$ mV). Under these conditions (Fig 4 B, open circles), the R663H-associated current showed the same voltage dependence, amplitude, and directionality as in Fig 2, as would be anticipated, since the transmembrane proton gradient is identical despite other differences in the recording solutions. If protons are the dominant charge carriers, the predicted consequence of a positive shift in E_{H+} is an increase in the R663H leak current density relative to that recorded in a symmetric proton gradient, due to an augmented inward proton driving force at the hyperpolarized voltages where opening of the R663H conductance is favored. As E_{H+} in both conditions is depolarized relative to the voltage range at which the R663H conductance is open (e.g. <-40 mV), both currents would be expected to be directed inwardly and exhibit the same voltage dependence. E_{H+} was shifted to $\sim+93$ mV by buffering the internal pH to 9.0. An increase in the normalized R663H-associated current was indeed observed under these conditions (Fig 4 B, filled circles), whereas there was no change in the leak conductance in oocytes expressing WT channels. As anticipated, the directionality and voltage dependence of the leak currents were unchanged. These results provided strong support for the notion that protons are the charge carriers of the R663H-associated leak.

To confirm that protons are the permeant species, we sought to shift E_{H+} to a sufficiently negative value to direct outward current though the R663H conductance (e.g., to induce an outward proton driving force at voltages where the R663H leak conductance is open). To accomplish this, the internal proton concentration was raised by buffering the intracellular pH to 5.0, shifting E_{H+} to ~-140 mV. Under these conditions, the R663H-specific current was outward with an apparent reversal potential approaching the predicted value of -140 mV (Fig. 5, A and B). The small current exhibited by WT-expressing oocytes was not significantly different from the nonspecific leak in mock-injected oocytes.

Consistent with previous experiments, the outward R663H proton conductance in Fig. 5 (A and B) was maximally open in the hyperpolarized range where the inward, resting conformation of the DIIS4 segment is favored. However, the gating transition between open (conducting) and closed (nonconducting) states was made more apparent when the proton current was directed

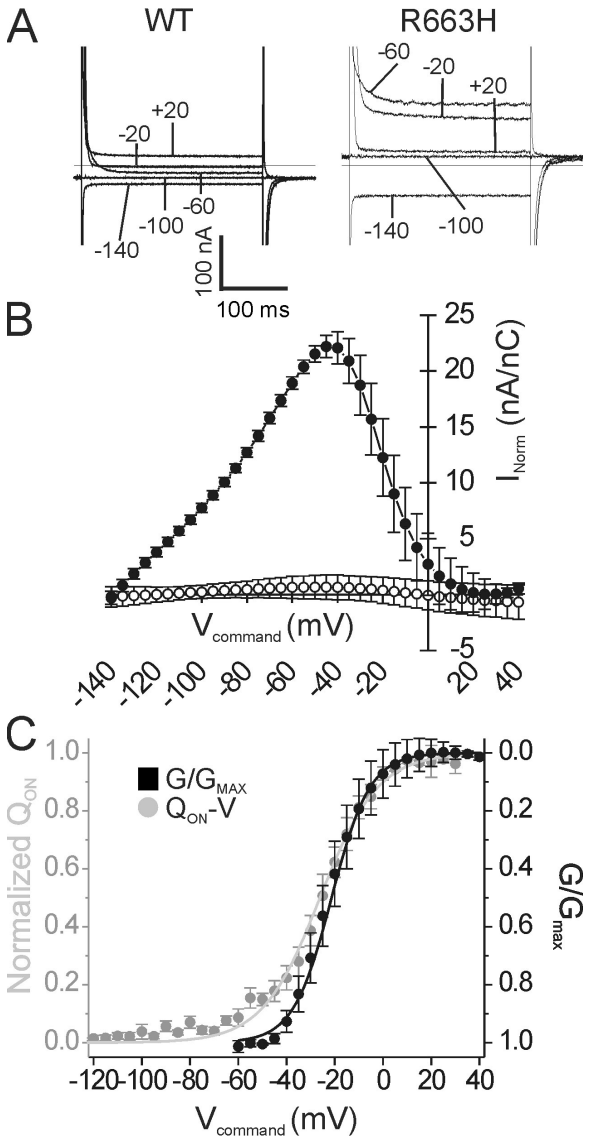

Figure 5. Intracellular acidification promotes outward proton current via the R663H gating-pore. To elicit an outward current through the R663H gating-pore, E_{H+} was shifted to ~−140 mV by buffering the cytoplasmic pH to ~5.0, while the external pH was maintained at 7.4. Representative raw current traces are shown in A, for oocytes expressing WT or R663H channels (denoted at top). Command voltages eliciting individual current responses are indicated (in mV) in the figures. Outward R663H gating pore currents are evident. After subtraction of the nonspecific leak derived from pooled data from mock-injected oocytes recorded under the same ionic conditions, and normalization to maximal Q_{On}, the corresponding current–voltage relationships for R663H (closed circles, $n = 5$) and residual WT (open circles, $n = 4$) currents are shown in B. In C, the normalized conductance–voltage relationship of the R663H gating-pore proton current (black circles, note inverted scale on the right) is compared with the R663H Q_{On}–voltage relationship derived from the same population of oocytes (gray circles). Both datasets are fit with Boltzmann functions yielding the following values: $G_{H+,(V)}$, $V_{1/2} = -21.3 \pm 3.9$ mV, $k = -8.0 \pm 2.1$ mV; $Q_{On,(V)}$, $V_{1/2} = -26.1 \pm 2.5$ mV, $k = 12.0 \pm 1.3$ mV ($n = 5$ for both sets).

outward (the sigmoidal portion of the $I_{(V)}$ relationship), providing an opportunity to assess the voltage dependence of this transition. Using the data in Fig. 5 B, the normalized conductance–voltage ($G_{(V)}$) relationship for the R663H proton conductance (between −80 and +30 mV) was computed. This relationship reflects the relative open probability of the proton leak conductance over this voltage range. Fig. 5 C demonstrates that this normalized $G_{(V)}$ curve is comparable to the voltage dependence of rNaV1.4-R663H Q_{On} displacement ($Q_{On(V)}$) recorded in the same transmembrane pH gradient. The overall right shift of the $Q_{On(V)}$ relationship in these experiments compared with those in Fig. 1 probably reflects alteration of voltage-sensing charges in contact with the acidified cytoplasmic compartment. Thus, the open probability of the R663H proton conductance closely tracks the voltage dependence of total gating charge movement, consistent with the notion that the proton conductance is gated by translocation of a single voltage sensor (e.g., DIIS4).

DISCUSSION

This report describes a novel physiological abnormality in a Na^+ channel mutation that causes human HypoPP (rNaV1.4-R663H). The mutation permits a low amplitude proton conductance via an accessory permeation pathway separate from the central Na^+ channel pore. Furthermore, the R663H-associated conductance exhibited a well-defined selectivity for protons over other physiologically abundant cations. Although the possibility exists that this proton conductance arises due to structural changes occurring elsewhere in the channel by allosteric perturbation, these results are most consistent with protons flowing through an exposed transmembrane crevice unblocked by the substitution of the DIIS4 charged side chain.

The ionic selectivity and voltage dependence of the R663H gating-pore current is consistent with results reported from missense substitution studies of the voltage-sensing domain of the *Shaker* K^+ channel. Starace and Bezanilla reported that histidine substitution at several charged S4 sites in *Shaker* channels creates proton permeation pathways with different voltage dependence characteristics depending on the site of mutation (Starace et al., 1997; Starace and Bezanilla, 2001, 2004). Tombola et al. (2005) further established that, whereas substitution of many of these same *Shaker* sites with other amino acid moieties permitted permeation of larger monovalent cations, no permissiveness for cations other than H^+ was observed after histidine substitution. Moreover, the voltage dependence of the R663H proton leak reported here follows an emerging pattern of gating-pore conductances wherein perturbations of extracellularly oriented sites in S4 segments establish permeation pathways opened by membrane hyperpolarization. Conversely, mutations in the

inner sites result in depolarization-activated conductances. With respect to NaV1.4, our data therefore support a structural model in which the outermost charged residue of the DIIS4 voltage sensor maintains aqueous contact with both extracellular and cytoplasmic compartments while the voltage sensor is in the "inward" conformation favored by hyperpolarization. This suggests that the DIIS4 gating crevice is constricted near this residue but not elsewhere, and that during activation, the R663 site is displaced from this local constriction.

Recently, gating-pore currents in three NaV1.4 HypoPP mutations have been reported by Sokolov et al. (2007). It was demonstrated that the mutation R666G in rNaV1.4 exposes a leak conductance favored by hyperpolarization. The aqueous pathway thus established was permissive for Na^+ and K^+, although both TEA^+ and $NMDG^+$ exhibited a low permeability as well. The amplitude of the R666G cation current was ~1.25% the amplitude of peak ionic currents, and is thus at least 10-fold higher than the R663H proton current we report here. These differences are unlikely to be explained by the differences in ionic constituents of the recording solutions, notably, Mg^{2+}-free bathing solution and a predominantly K^+-based internal solution in Sokolov et al. In experiments not shown, we confirmed that the presence of internal K^+ did not alter the amplitude of the R663H proton current. Furthermore, differences in the leak correction methodology between the present report and that of Sokolov et al. are insufficient to account for a >10-fold difference in current amplitude. Instead, the difference in gating-pore current amplitudes is most likely due to differences in the structural conformation between the R666G and R663H permeation pathways. The authors also report a hyperpolarization-activated inward current arising from R663H channels, the mutation studied herein, which they interpreted as a Na^+-permissive conductance. However, an investigation of the ionic selectivity of the R663H current they detected was not reported, nor was the amplitude of the R663H current relative to ionic or gating currents studied. It is therefore not clear if the inward current identified by Sokolov et al. is identical to the R663H gating-pore conductance in the present report. The currents the authors demonstrated can be equally attributed to proton permeation, as both protons and Na^+ ions would be subject to an inward driving force at hyperpolarized voltages, given the symmetrical pH gradient described in their experiments.

It is possible that the gating pore leaks described here and by Sokolov et al. are merely epiphenomena of the disease mutations with no pathophysiological significance. The growing number of HypoPP mutants associated with aberrant inward currents at hyperpolarized potentials, however, lends support to the hypothesis that gating-pore currents may be the pathogenetic determinant. More informed analysis as to the potential relevance of these aberrant gating-pore leaks will require establishing what features are shared by aberrant currents mediated by different HypoPP mutations. Our data narrow these possibilities, as the R663H gating-pore exhibited unique selectivity for protons over other physiologically abundant cations. Given the likelihood that voltage-sensing domains in different channels maintain a homologous structural topology, it is not surprising that proton permeation similar to that exhibited by *Shaker* K^+ channel histidine mutants can be demonstrated in NaV1.4 histidine substitutions causing HypoPP, and likely also exist for histidine substitutions in CaV1.1. In light of this, it is reasonable to consider the possibility that proton permeation specifically, irrespective of the permeability of other cations, might be the essential pathophysiological component of a HypoPP gating-pore current.

What inferences can be drawn about the physiological effects of the NaV1.4-R663H gating-pore proton conductance, which might support the plausibility of its role in the pathogenesis of HypoPP? The internal pH of quiescent skeletal muscle is maintained at an estimated 0.2–0.3 pH units less than extracellular pH (Adler et al., 1965). Although this concentration gradient for protons favors outward flux with E_{H+} maintained between −6 and −20 mV, this reversal potential is well depolarized from normal muscle V_{REST} of −85 mV. Consequently, skeletal muscle harboring the R663H mutation would experience a sustained inward proton leak due to this electromotive force. Using the data from R663H mutant as an example, the magnitude of this aberrant proton leak in mature muscle can be estimated. At −85 mV, the normalized chord conductance of the R663H proton current is 0.15 μS/nC, equivalent to a unitary gating-pore conductance of 1.7×10^{-4} pS. Given estimates of ~500 Na^+ channels/μm^2 of sarcolemma in mature muscle (Bay and Strichartz, 1980), a total proton conductance of ~4.3 $\mu S/cm^2$ would be predicted in heterozygotic fibers. This is well below measured values of resting membrane K^+ and Cl^- conductances (200–300 $\mu S/cm^2$), which maintain V_{REST} under normal conditions (Lipicky et al., 1971; Kwiecinski et al., 1984). Thus, although the R663H proton leak is likely to command a degree of sarcolemmal depolarization, it is probably insufficient to account for depolarization of >20 mV during a paralytic attack.

Nevertheless, it is possible that a persistent inward proton leak of this magnitude might have an important pathophysiological impact indirectly, via effects on intracellular pH. Myoplasmic compensation for an aberrant sarcolemmal proton conductance likely involves a complex interaction between intracellular proton diffusion, proton buffering, and active proton extrusion (Kemp et al., 1993; Swietach et al., 2005). From the above estimates, R663H heterozygotic muscle is subject to a proton influx of $\sim 3.3 \times 10^{-12}$ M s^{-1} per cm^2 traversing the mutant voltage sensor. In comparison, ^{31}P-MRS

studies estimate that the sarcolemma has the capacity to extrude protons at rates up to 1.67×10^{-7} M s^{-1} per cm^3 in response to intracellular acidification associated with peak exercise (Kemp et al., 1993). Given a rough estimate of the surface-to-volume ratio of $2/r$, where r is the radius of the fiber (and discounting the T-tubule system for simplicity), this maximal extrusion rate is about two orders of magnitude greater than the R663H-associated inward proton leak, in a typical fiber of 100 μM diameter. Active proton extrusion under resting conditions, however, is much lower, comparable in magnitude to the predicted influx through the R663H gating-pore (Kemp et al., 1993). Thus, the R663H proton conductance may be sufficiently large to impair myoplasmic pH homeostasis. This conservative estimate discounts the potential contribution of the T-tubular system to membrane area, which, if taken into account, would dramatically increase the ratio between R663H-mediated proton influx and proton extrusion. The effect of this sustained proton load may be acidification of the bulk myoplasm, or even creation of an acidified subsarcolemmal microdomain, which in turn may have important consequences for the function of sarcolemma K^+ and Cl^- conductances maintaining V_{REST}. Alternatively, a sustained proton leak might reduce myoplasmic buffering capacity, leading to abnormalities in handling additional physiological proton loads, such as during recovery from peak exercise.

Our data define a novel physiological abnormality associated with mutations linked to HypoPP, which may be the pathogenetic mechanism whereby these mutations are coupled to the phenotype of episodic paralysis. The notion that an aberrant proton conductance might contribute to the pathophysiology of HypoPP would be buttressed by finding similar proton conductances caused by other HypoPP mutations in both NaV1.4 and CaV1.1 channels.

This work was supported by grants from the Muscular Dystrophy Association (MDA4030 AFS), and National Institutes of Health/National Institute of Arthritis and Musculoskeletal and Skin Diseases (AR42703 SCC).

Olaf S. Andersen served as editor.

Submitted: 30 January 2007
Accepted: 18 May 2007

REFERENCES

Adler, S., A. Roy, and A.S. Relman. 1965. Intracellular acid-base regulation. I. The response of muscle cells to changes in Co2 tension or extracellular bicarbonate concentration. *J. Clin. Invest.* 44:8–20.

Armstrong, C.M., and F. Bezanilla. 1974. Charge movement associated with the opening and closing of the activation gates of the Na channels. *J. Gen. Physiol.* 63:533–552.

Bay, C.M., and G.R. Strichartz. 1980. Saxitoxin binding to sodium channels of rat skeletal muscles. *J. Physiol.* 300:89–103.

Bulman, D.E., K.A. Scoggan, M.D. van Oene, M.W. Nicolle, A.F. Hahn, L.L. Tollar, and G.C. Ebers. 1999. A novel sodium channel mutation in a family with hypokalemic periodic paralysis. *Neurology.* 53:1932–1936.

Cannon, S.C. 2006. Pathomechanisms in channelopathies of skeletal muscle and brain. *Annu. Rev. Neurosci.* 29:387–415.

Carle, T., L. Lhuillier, S. Luce, D. Sternberg, O. Devuyst, B. Fontaine, and N. Tabti. 2006. Gating defects of a novel Na^+ channel mutant causing hypokalemic periodic paralysis. *Biochem. Biophys. Res. Commun.* 348:653–661.

Catterall, W.A. 1995. Structure and function of voltage-gated ion channels. *Annu. Rev. Biochem.* 64:493–531.

Cha, A., P.C. Ruben, A.L.J. George, E. Fujimoto, and F. Bezanilla. 1999. Voltage sensors in domains III and IV, but not I and II, are immobilized by Na^+ channel fast inactivation. *Neuron.* 22:73–87.

Jurkat-Rott, K., F. Lehmann-Horn, A. Albaz, R. Heine, R.G. Gregg, K. Hogan, P.A. Powers, L. P., J.E. Vale-Santos, J. Weissenback, and B. Fontaine. 1994. A calcium channel mutation causing hypokalemic periodic paralysis. *Human Molecular Genetics.* 3:1415–1419.

Jurkat-Rott, K., N. Mitrovic, C. Hang, A. Kouzmekine, P. Iaizzo, J. Herzog, H. Lerche, S. Nicole, J. Vale-Santos, D. Chauveau, et al. 2000. Voltage-sensor sodium channel mutations cause hypokalemic periodic paralysis type 2 by enhanced inactivation and reduced current. *Proc. Natl. Acad. Sci. USA.* 97:9549–9554.

Kemp, G.J., D.J. Taylor, P. Styles, and G.K. Radda. 1993. The production, buffering and efflux of protons in human skeletal muscle during exercise and recovery. *NMR Biomed.* 6:73–83.

Kuzmenkin, A., V. Muncan, K. Jurkat-Rott, C. Hang, H. Lerche, F. Lehmann-Horn, and N. Mitrovic. 2002. Enhanced inactivation and pH sensitivity of Na^+ channel mutations causing hypokalaemic periodic paralysis type II. *Brain.* 125:835–843.

Kwiecinski, H., F. Lehmann-Horn, and R. Rüdel. 1984. The resting membrane parameters of human intercostal muscle at low, normal, and high extracellular potassium. *Muscle Nerve.* 7:60–65.

Lapie, P., C. Goudet, J. Nargeot, B. Fontaine, and P. Lory. 1996. Electrophysiological properties of the hypokalaemic periodic paralysis mutation (R528H) of the skeletal muscle α1s subunit as expressed in mouse L cells. *FEBS Lett.* 382:244–248.

Lerche, H., N. Klugbauer, F. Lehmann-Horn, F. Hofmann, and W. Melzer. 1996. Expression and functional characterization of the cardiac L-type calcium channel carrying a skeletal muscle DHP-receptor mutation causing hypokalaemic periodic paralysis. *Pflugers Arch.* 431:461–463.

Liman, E.R., J. Tytgat, and P. Hess. 1992. Subunit stoichiometry of a mammalian K^+ channel determined by construction of multimeric cDNAs. *Neuron.* 9:861–871.

Lipicky, R.J., S.H. Bryant, and J.H. Salmon. 1971. Cable parameters, sodium, potassium, chloride, and water content, and potassium efflux in isolated external intercostal muscle of normal volunteers and patients with myotonia congenita. *J. Clin. Invest.* 50:2091–2103.

McClatchey, A.I., S.C. Cannon, S.A. Slaugenhaupt, and J.F. Gusella. 1993. The cloning and expression of a sodium channel β1-subunit cDNA from human brain. *Hum. Mol. Genet.* 2:745–749.

Morrill, J.A., R.H. Brown Jr., and S.C. Cannon. 1998. Gating of the L-type Ca channel in human skeletal myotubes: an activation defect caused by the hypokalemic periodic paralysis mutation R528H. *J. Neurosci.* 18:10320–10334.

Ptacek, L.J., R. Tawil, R.C. Griggs, A.G. Engel, R.B. Layzer, H. Kwiecinski, P.G. McManis, L. Santiago, M. Moore, G. Fouad, et al. 1994. Dihydropyridine receptor mutations cause hypokalemic periodic paralysis. *Cell.* 77:863–868.

Sokolov, S., T. Scheuer, and W.A. Catterall. 2005. Ion permeation through a voltage-sensitive gating pore in brain sodium channels having voltage sensor mutations. *Neuron.* 47:183–189.

Sokolov, S., T. Scheuer, and W.A. Catterall. 2007. Gating pore current in an inherited ion channelopathy. *Nature*. 446:76–78.

Starace, D.M., and F. Bezanilla. 2001. Histidine scanning mutagenesis of basic residues of the S4 segment of the shaker K^+ channel. *J. Gen. Physiol.* 117:469–490.

Starace, D.M., and F. Bezanilla. 2004. A proton pore in a potassium channel voltage sensor reveals a focused electric field. *Nature*. 427:548–553.

Starace, D.M., E. Stefani, and F. Bezanilla. 1997. Voltage-dependent proton transport by the voltage sensor of the Shaker K^+ channel. *Neuron*. 19:1319–1327.

Sternberg, D., T. Maisonobe, K. Jurkat-Rott, S. Nicole, E. Launay, D. Chauveau, N. Tabti, F. Lehmann-Horn, B. Hainque, and B. Fontaine. 2001. Hypokalaemic periodic paralysis type 2 caused by mutations at codon 672 in the muscle sodium channel gene SCN4A. *Brain*. 124:1091–1099.

Struyk, A.F., K.A. Scoggan, D.E. Bulman, and S.C. Cannon. 2000. The human skeletal muscle Na channel mutation R669H associated with hypokalemic periodic paralysis enhances slow inactivation. *J. Neurosci.* 20:8610–8617.

Swietach, P., C.H. Leem, K.W. Spitzer, and R.D. Vaughan-Jones. 2005. Experimental generation and computational modeling of intracellular pH gradients in cardiac myocytes. *Biophys. J.* 88:3018–3037.

Tombola, F., M.M. Pathak, and E.Y. Isacoff. 2005. Voltage-sensing arginines in a potassium channel permeate and occlude cation-selective pores. *Neuron*. 45:379–388.

Trimmer, J.S., S.S. Cooperman, S.A. Tomiko, J.Y. Zhou, S.M. Crean, M.B. Boyle, R.G. Kallen, Z.H. Sheng, R.L. Barchi, F.J. Sigworth, et al. 1989. Primary structure and functional expression of a mammalian skeletal muscle sodium channel. *Neuron*. 3:33–49.